# Predicting Phase Resetting Due To Multiple Stimuli

**Kelsey M. Vollmer, Davy C. Vanderweyen, Derek R. Tuck, and Sorinel A. Oprisan***

***College of Charleston, Charleston, SC***

We generalized the phase resetting curve (PRC) to a more realistic case of neural oscillators receiving two or more inputs per cycle. The PRC tabulates the transient change in the firing period of a neuron due to an external perturbation, such as a presynaptic stimulus. We used a conductance-based model neuron to estimate experimentally the two-stimulus PRC and compared the results against our mathematical prediction based on the assumption of instantaneous recurrent stimulation. Within the limits of the recurrent stimulation assumptions, we found that the newly introduced prediction for the two-stimulus PRC matched experimental measurements. Our new results open the possibility of a more realistic approach to predicting phase-locked modes in neural networks, such as the synchronous activity of large networks during epileptic seizures..

## Introduction

Neurons are excitable cells capable of generating large membrane potential excursions when electrically or chemically stimulated [1,4,5]. Hodgkin and Huxley modeled the electrical activity of excitable cells using only two main ionic species: sodium and potassium [4,5]. The extracellular environment of neurons is rich in sodium ions (≈ 440 mM/L) and relatively low in potassium (≈ 20 mM/L). The intracellular concentrations are inverted, i.e. only about 60 mM/L for sodium ($Na^+$) and about 400 mM/L for potassium ($K^+$) [1,4,5]. Due to the strong concentration gradient of $Na^+$, it tends to flow inside the cell if ionic channels (pores in the cell membrane) allow it. The strength of $Na^+$ electrochemical flow is measured by Nernst's potential, which is about +50 mV [4,5]. The positive sign indicates an inward flow of $Na^+$ ions. For $K^+$ ions, the electrochemical potential is about -90 mV, where the negative sign indicates an outward flow. Since the neurons usually have more potassium than sodium channels expressed per unit area, the equilibrium (or rest) potential of the cell is around -65 mV, i.e. closer to Nernst's potential of $K^+$ than to $Na^+$ [5]. At rest, both $K^+$ and $Na^+$ ions constantly flow in and out of the cell down their electrochemical gradients through non-specific channels called leak channels [5]. The ion channels are integral membrane proteins that can change their conformation in response to electric pulses and allow ions to enter or exit a cell. There are many types of ion channels that respond to various stimuli, such as pressure-sensitive channels which respond to mechanical stimuli [2], ligand-gated channels that respond to specific extracellular ligand molecules [12], or voltage-gated ion channels which open in response to a change in the electric potential difference across the cell membrane [5].

An action potential (AP) is a significant excursion in the membrane potential difference due to the activation of voltage-gated ionic channels. At rest, the fraction of active voltage-gated channels is relatively small. However, a positive external electrical stimulation (excitation), e.g. stimuli coming from other excitable cells, could produce a slight increase in the membrane potential of the cell. As a result, voltage-gated $Na^+$ channels, which are very sensitive to any increase (depolarization) in membrane potential, open immediately and allow an influx of $Na^+$. This influx of positive charges further depolarizes the cell, which results in the opening of more voltage-gated $Na^+$ channels; this process could produce an avalanche that reaches a critical excitability threshold. (see Fig. 1a). At the threshold, which is around -55 mV (Fig. 1a), the cell is in an unstable state and a slight depolarization produces an exponential increase in the number of $Na^+$ channels that open. As a result, the $Na^+$ flow of positive ions would push the membrane potential towards Nernst's potential of $Na^+$ (see the upstroke of AP in Fig. 1a). The membrane potential reaches about +40 mV over 1-2 ms and produces a spike of electrical activity (see Fig. 1a).

Voltage-gated $K^+$ channels also activate (open) in response to depolarizations. However, $K^+$ channels are slower than $Na^+$ channels. As a result, they would significantly contribute to an AP only after the membrane potential already reached the highest depolarization of about +40 mV. Once potassium channels open, they allow an outward flow of $K^+$, which pushes the membrane potential towards the Nernst's potential of $K^+$. Additionally, after 1-2 ms, sodium channels inactivate, blocking further $Na^+$ influx. The inactivation of sodium channels combined with the slow activation of potassium channels leads to cell repolarization (see the downstroke of the AP in Fig. 1a). After every AP, the ionic balance of a cell is perturbed and the $Na^+/K^+$ pump works against the concentration gradients to reestablish the normal ionic concentrations. The $Na^+/K^+$-ATP pump constantly moves 3 $Na^+$ ions out and brings 2 $K^+$ ions into the cell during every pump cycle [5].

The above-described mechanism is the foundation of any conductance-based, or Hodgkin-Huxley (HH), model of excitable cells. Some more realistic models also consider other ionic currents involved in generating an AP, e.g. calcium, chlorine, magnesium, etc. Furthermore, each ionic species has multiple ion channel (proteins) types that can actively transport them across the membrane. For example, there are over twenty different types of potassium channels, some of them do not inactivate (as above), some inactivate (like sodium channels), and some require $Ca^{2+}$ or $Mg^{2+}$ presence to function [5]. Hodgkin and Huxley showed experimentally that despite the wide variety of morphologies, ion channel types, and AP shapes, there are only two classes of excitable cells that produce oscillatory activities [1,4]. Type I excitability class refers to neurons that can fire an AP of arbitrarily low frequency in response to an externally injected bias current (Fig. 1b – solid circles), whereas type II neurons can only oscillate above a critical frequency (Fig. 1b – solid squares). All excitable cells are nonlinear systems that work close to the stability threshold

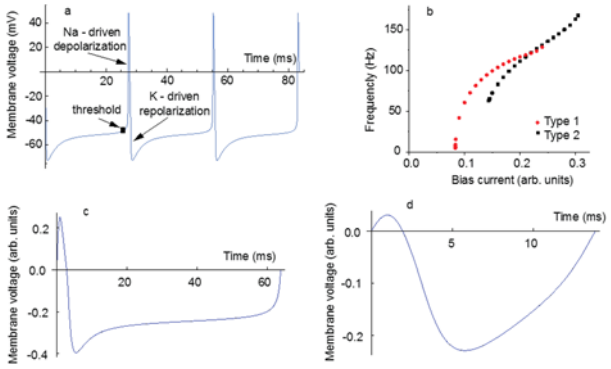


Figure 1. An action potential generated by the influx of $Na^+$ (upstroke) and the repolarization due to $K^+$ outflow (a). The resting membrane potential is determined by the conductance of leakage current and the activity of $Na^+/K^+$-ATP pump. (b) Frequency versus steady stimulus current (f-I) curves show two distinct responses. Type I excitable cells fire with arbitrarily low frequency (solid circles), whereas type II cells can only fire above a critical frequency (solid squares). Typical AP generated by type I (c) and type II (d) model neurons.

(see Fig. 1a). Although the excitability class is determined by the type of instability near the AP threshold [1,7,11,14,15], qualitative differences between the two types are also visible in the shape of the AP. Type I excitability class has a very brief AP followed by a relatively long silent period (Fig. 1c) whereas type II excitability shows an almost sinusoidal AP (Fig. 1d).

**Phase Resetting Curve**

The phase resetting curve (PRC) theory reduces the complexity of the ionic mechanisms involved in generating APs to measuring the response of the neurons to a brief perturbation applied at different phases during a cycle of activity [13]. The PRC is a graphical representation of the advances or delays of the subsequent spike produced by a perturbation, e.g. a presynaptic input from another neuron (Fig. 2) [3,8,9,13].

Instead of focusing on a detailed and biologically accurate description of AP mechanisms and how presynaptic stimuli change the response of a neuron, the PRC treats the cell as a functional unit characterized by an input-output transfer function, i.e. the PRC tabulates the relative change in the firing period of the cell for inputs delivered at different times (phases) during the ongoing periodic activity.

If a stable oscillatory neural activity exists (see Fig. 3a – continuous line), then a phase variable could be unambiguously defined as the normalized stimulus time ($t_s$) with respect to the intrinsic period of oscillation ($P_i$), i.e. $\varphi = t_s/P_i$. The first order transient phase resetting is defined by (see Figs. 2a and 2c) [10]:

$$F(\varphi) = 1 - P_1/P_i = \Delta P_1/P_i, \quad (1)$$

and measures the relative advance, $\Delta P_1 = P_i - P_1 > 0$, or delay, $\Delta P_1 = P_i - P_1 < 0$, of the subsequent spike induced by an incoming input at phase $\varphi = t_s/P_i$.

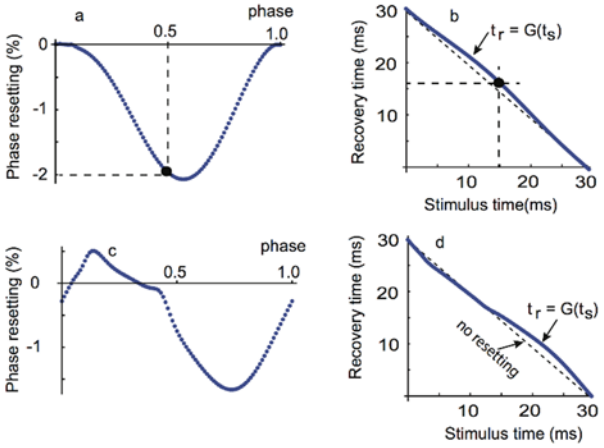


Figure 2. Type I neurons produce unimodal PRCs (a) whereas type II neurons produce bimodal PRCs (c). The corresponding spike time response curves (STRCs) plot the time it takes a neuron to respond to a perturbation (the response or recovery time, tr) versus the stimulus time, ts, of a neuron. The STRCs and the first order PRC contain similar information, although for predicting the phase-locked modes of a network it is graphically more intuitive to use STRCs [9,11].

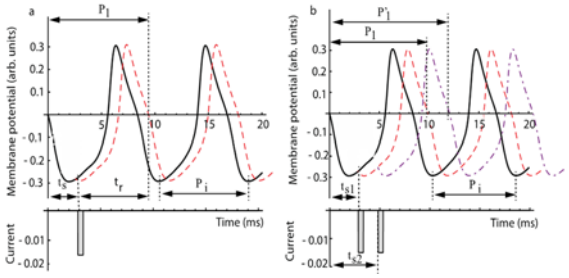


Figure 3. Single-stimulus (a) and two-stimulus (b) PRC protocol measures the final transient change in the firing period of a neural oscillator. In the single-stimulus PRC, the transient change is $\Delta P = 1 - P_1/P_i$ due to a stimulus applied at phase $\varphi_1 = t_s/P_i$. In the two-stimulus cased (b), the first stimulus at $t_{s1}$ changes the firing period from $P_i$ to $P_1$ and the second stimulus, arriving at $t_{s2}$, further changes it to $P_1$'. The total phase resetting is $\Delta P = 1 - P'_1/P_i$.

Alternatively, resetting induced by an incoming stimulus at stimulus time, $t_s$, could be tabulated in terms of neural oscillator's response, or recovery, time $t_r$ in open loop (see Fig. 3a) [8,11]:

$$t_r = G(t_s), \quad (2)$$

Figure 2 shows that a stimulus applied at phase $\varphi = 0.5$ changes the intrinsic period of neuronal oscillation from $P_i = 30$ ms to $P_1 = 30.6$ ms, i.e. a phase resetting $\Delta P_1$ of -2% of $P_i$ (the negative sign indicates a delay of the subsequent spike). The plot of phase change, $F(\varphi)$ given by Eq. (1), as a function of the stimulus phase, $\varphi = t_s/P_i$, generates the PRCs shown in Figs. 2a and 2c. Based on Fig. 3a, the recovery time, $t_r$, and the transiently modified firing

period $P_1$ are related by:

$$P_1 = t_s + t_r \Rightarrow \quad t_r = P_1 - t_s. \tag{3}$$

Using the definition (1) of the PRC, it results that:

$$P_1 = (1 - F(\varphi))P_i = (1 - F(t_s/P_i))P_i, \tag{4}$$

which substituted into (3) leads to:

$$t_r = (1 - F(t_s/P_i))\, P_i - t_s = G(t_s). \tag{5}$$

Both type I (Fig. 2b) and type II (Fig. 2d) STRCs carry out the same information as the corresponding PRCs. For example, a stimulus delivered to a neural oscillator with intrinsic firing period $P_i = 30$ ms at phase $\varphi = 0.5$ in Fig. 2a has a corresponding stimulus time $t_s = 15$ ms. According to the corresponding STRC (see Fig. 2b), its recovery time $t_r = 15.6$ ms, which leads to the same transiently modified period $P_1 = 30.6$ ms as we determined using the PRC.

The advantage of the PRC method is that it allows theoretical predictions regarding the existence and stability of phase-locked modes starting from known differential [14] or difference equations for model neurons (a subject that is outside the scope of this paper). Another important advantage of the PRC method is that it can be easily generated experimentally in any neurophysiology lab [3,8,14,16].

In this paper, we relaxed one of the strong restrictions on using the PRC, i.e. the requirement that the open-loop PRC is generated in response to only one stimulus per cycle (see Fig. 3). Although PRCs in response to isolated stimuli are very useful, for example, in predicting the 1:1 phase-locked modes in neural networks of invertebrates (see [8,9,10,11] and references therein), they have limited use in studying vertebrates brain due to the very large number (of the order of thousands [5]) of (almost) simultaneous inputs a cortical neuron receives during each cycle. In this paper, we used recursive functions to predict the response of a computational model to two inputs per cycle and compare the prediction against actual numerical data. Our approach is general and could be extended to any number of inputs per cycle to mimic biological-relevant activity of neural cells.

## Methods

### The Computational Model

We used a conductance-based computational model to generate all PRCs and to test all our hypotheses. The archetypical conductance-based model was introduced by Hodgkin and Huxley (HH) [4] and only involves $Na^+$ and $K^+$ ionic currents as briefly described in the Introduction section. In this paper, we used a Morris-Lecar (ML) model because it allowed us to switch its behavior from a type I to a type II excitable class by adjusting a relatively small number of parameters [1,7]. In contrast, HH model cannot switch between excitability classes [1]. The added flexibility of the ML model is due to a different, albeit biologically relevant, dynamics that replicates the calcium and potassium oscillations in the muscle fiber of a giant barnacle [7]. The general mathematical equation of any conductance-based model neuron is:

$$C_m\, dV/dt + \Sigma\, I = 0, \tag{5}$$

where $C_m$ is the membrane capacitance, V is the membrane voltage, $C_m$ dV/dt is the capacitive current due to membrane polarization, and $\Sigma$ I stands for the sum of all other ionic currents flowing in and out of the cell. In particular, for ML model neuron the currents involved are

$$C_m\, dV/dt + I_{Ca} + I_K + I_{leak} + I_{bias} = 0, \tag{6}$$

where $I_{Ca}$ is the inwards calcium current, $I_K$ is the outward potassium current, $I_{leak}$ is the nonspecific (leakage) ionic current responsible for the rest membrane potential, and $I_{bias}$ is any non-intrinsic (external) current, such as the presynaptic inputs or external stimuli through electrodes inserted into the cell. The ionic currents are described by Ohm's law [1,5]:

$$I = g\,(V - E), \tag{7}$$

where g is the electrical conductance of the membrane and E is the reverse (Nernst) electrochemical potential of a specific ion channel. For leakage channels the conductance is just a constant. However, the conductance of active ionic channels, such as calcium and potassium is voltage-dependent with very strong nonlinearities. For example, the complete equations of ML model are:

$$C_m\, dV/dt + g_{Ca}\, m_\infty\, (V - E_{Ca}) + g_K\, w\, (V - E_K) + g_{leak}\, (V - E_{leak}) + I_{bias} = 0, \tag{8a}$$

$$dw/dt = \phi\, (w_\infty - w)/\tau_w, \tag{8b}$$

where w represents the fraction of potassium channels open at any given time, $m_\infty = 0.5(1 + \tanh((V - V_1)/V_2))$ is the steady-state fraction of calcium channels open at a given voltage V, $w_\infty = 0.5(1 + \tanh((V - V_3)/V_4))$ is the steady-state fraction of potassium channels open at a given voltage V, and the characteristic time constant of potassium channels is $\tau_w = 1/\cosh((V - V_3)/2V_4))$. All ML model parameters are dimensionless, i.e. the voltages were divided by calcium Nernst's potential of $E_{Ca} = 120$ mV, conductances were divided by potassium conductance of $g_K = 2$ $\mu S/cm^2$, the currents were divided by $g_K * E_{Ca} = 100$ $\mu A/cm^2$, the membrane capacitance $C_m = 5$ $\mu F/cm^2$, determines the time constant of the system $C_m/g_L = 2.5$ s. The dimensionless parameter for a ML model neuron are: $V_1 = -0.01$; $V_2 = 0.15$; $V_3 = 0.1/0.017$; $V_4 = 0.145/0.25$; $V_{Ca} = 1$; $V_K = -0.7$; $V_L = -0.5$; $g_{Ca} = 1.33/2.2$; $g_L = 0.5/1.0$; $g_K = 2.0/4.0$; $C_m = 1$; $\phi = 0.6/0.417$, and I = 0.0725/0.4 [1]. For example, potassium reversal $V_K = -07$ dimensionless units means $V_K = -0.7 * 120$ mV = -84 mV; $g_K = 2.0$ (type I)/4.0 (type II) means $g_K = 2.0 * 2$ $\mu S/cm^2$ (type I)/$4.0 * 2$ $\mu S/cm^2$ (type II) = 4.0 $\mu S/cm^2$ (type I)/8.0 $\mu S/cm^2$ (type II).

### PRC Generation

**Single-stimulus PRC.** We used Eqs. (8) to simulate neural activity with Mathematica software. The bias current $I_{bias}$ contained a continuous (dc) component that allowed stable oscillations with the intrinsic firing period of about $P_i = 8.5$ ms (see Fig. 3). On top of the dc component, we superimposed a brief rectangular current pulse of amplitude (A) and duration $\tau$ (see Fig. 3a). By measuring the transient change in the first firing period $P_1$ due to the stimulus applied at $t_s$ (Fig. 3a) we obtained the single-stimulus PRC (see Fig. 4a). In the case of a rectangular stimulus, the parameter space of a single-stimulus PRC is 3-dimensional, i.e. ($\varphi$, A, $\tau$). We often

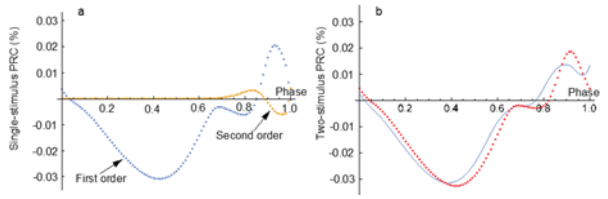


Figure 4. Experimentally measured single stimulus (a) and two-stimulus PRC (b). The experimental PRC (continuous line) and theoretically prediction (dotted lines) for a delay time $\Delta t$ =1% of $P_i$ between stimuli with amplitude A = -0.001 $\mu A/cm^2$ and duration $\tau$ = 1% of $P_i$.

represent the PRCs as a family of two-dimensional curves (see Fig. 4a) with the phase resetting $F(\varphi)$ along the vertical axis versus stimulus phase $\varphi$ along the horizontal axis for fixed values of (A, $\tau$).

**Two-stimulus PRC.** In a similar manner, we superimposed two identical rectangular pulses on the dc component of $I_{bias}$ (see Fig. 3b) to find the phase resetting induced by the train of pulses, such as synaptic inputs (see Fig. 4b). In the case of two-stimulus PRCs, the resetting depends not only on the phase $\varphi_1$ of the first stimulus, its amplitude A and duration $\tau$, but also o the delay time to the next rectangular input $\Delta t$. In the simplest case of two identical rectangular stimuli, the parameter space that defines a two-stimulus PRC is 4-dimensional, i.e. ($\varphi_1$, A, $\tau$, $\Delta t$). For geometrical convenience, the two-stimulus PRCs are two-dimensional families of curves $F(\varphi_1, \varphi_2)$ that depend on the phase of both the first and second stimulus (for a more precise definition see next section). The two-stimulus PRC, $F(\varphi_1, \varphi_2)$, is measured experimentally (see Fig. 3b) by recording the final transient change in the firing period due to both stimuli, i.e.

$$F(\varphi_1, \varphi_2) = 1 - P_1'/P_i. \quad (9)$$

## Results

### Theoretical model of two-stimuli PRC

According to the definition (1) of the singe-stimulus PRC, the transiently changed firing period of a neuron in response to the first stimulus arriving at stimulus time $t_{s1}$ (phase $\varphi_1 = t_{s1}/P_i$) is given by Eq. (4). As a result of the first stimulus, the second stimulus that arrived at $t_{s2} = t_{s1} + \Delta t$ finds a (transiently) modified firing period $P_1$ instead of $P_i$.

To predict the phase resetting induced by the second stimulus we made two assumptions: (1) instantaneous resetting, i.e. the effect of the first stimulus is consumed by the time the second stimulus arrives, and (2) the PRC scales with the firing period. The first assumption is necessary because it allows us to treat the second stimulus as if it acts alone on a neural oscillator with a (transiently modified) firing period $P_1$. Sometimes this assumption is also called memory-less process, although the memory of the first stimulus is present in the transiently modified firing period $P_1$. The second assumption is also necessary because it allows us to used over and over a scaled version of the single-stimulus PRC, $F(\varphi)$, to find the effect of multiple stimuli.

Based on the two assumptions, the second stimulus arrives at a stimulus time $t_{s2} = t_{s1} + \Delta t$, which corresponds to a phase

$$\varphi_2 = t_{s2}/P_1 = (t_{s1} + \Delta t)/((1 + F(\varphi_1))P_i). \quad (10)$$

Using recursively the definition provided by Eq. (4), we estimate that the new (transiently modified) firing period due to the second stimulus is:

$$P_1' = P_1 (1 - F(\varphi_2)) \quad (11)$$

Substituting (4) and (10) into (11) we get $P_1' = Pi\ (1 - F(\varphi_1))(1 - F(\varphi_2))$, which combined with the definition (9) gives the two-stimulus PRC $F(\varphi_1, \varphi_2)$ in terms of the single-stimulus PRC $F(\varphi)$:

$$1 - F(\varphi_1, \varphi_2) = (1 - F(\varphi_1))(1 - F(\varphi_2)). \quad (12)$$

Our theoretical prediction is that Eq. (12) represents a good approximation of the experimental two-stimulus PRC obtained using Eq. (9). Our prediction can also be generalized to an arbitrary number of stimuli, which opens the possibility of a more realistic use of PRC in predicting phase-locked modes in cortical circuits.

### Experimental validation of two-stimulus PRC model

We carried out measurements of single-stimulus (see Fig. 4a) and two-stimulus (see Fig. 4b) PRCs. The single-stimulus PRC was measured according to definition (1) and two-stimulus PRC was computed based on (9). The experimental two-stimulus PRC was compared against the theoretical predictions given by Eq. (12) and the sum of the squares of all differences between the two curves was computed, i.e. the prediction error. Typical results are shown in Fig. 4. We were interested in quantifying the goodness of our prediction based on Eq. (12) when compared against the experimental two-stimulus PRC computed according to definition (9). Since the parameter space is very high, we fixed the delay $\Delta t$ between the two stimuli to 1% of $P_i$ (Fig. 5a), respectively, 5% of $P_i$ (Fig. 5b) while scanning a wide range of amplitudes and pulse durations. We found that the contour levels of constant percent error follow arcs of hyperbolae (see continuous black lines in Fig. 5).

Since in the plane of amplitude versus stimulus duration the product amplitude*duration is constant along a hyperbola, it results that the amplitude and duration of a stimulus have similar effect on phase resetting. This is because for a rectangular current stimulus, the product amplitude*duration represents the amount of injected electric charge into the cell due to the external perturbation. Our findings suggest that doubling the amount of phase resetting could be achieved either by doubling the duration of the stimulus or by doubling its amplitude, which both inject the same amount of electric charge into the cell. Obviously, such a linear relationship and equivalence of amplitude and duration of stimulus fails for large durations and/or amplitudes.

Another relevant result of our study is that closely spaced stimuli (Fig. 5a) lead to larger prediction errors than stimuli spaced farther from each other (Fig. 5b). The reason is that, in the case of closely spaced stimuli, the neuron did not have enough time to recover from the previous inhibition and the figurative point was not yet back on the unperturbed limit cycle. As a result, there is a large error in estimating the phase of the second stimulus, which leads to larger overall error of PRC prediction.

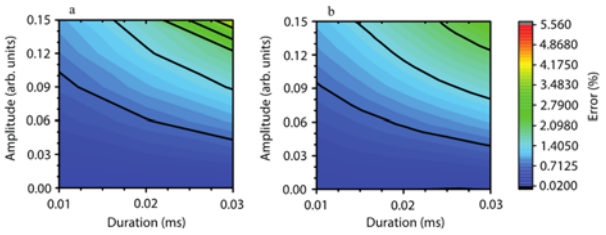


Figure 5. The error between the experimental and theoretical two- stimulus PRC increased with the amplitude and duration of the stimulus. For a short delay time of 1% of $P_i$ (a), the error increases more rapidly than for a larger 5% of $P_i$ (b) delay time between stimuli. The continuous black curves mark levels of constant injected electric charge, i.e. stimuli for which the area of the current stimulus is constant.

## Discussion

Our goal is to understand how neurons exchange information and how that process leads to neural networks organization. For this purpose, simple lookup tables, or PRCs, that map the timing (or phase) of the incoming stimulus to relative change in firing period (phase resetting) suffice.

In this paper, we generalized the single-stimulus PRC theory to multiple stimuli per cycle in order to correctly apply PRC method to cortical neural networks that have highly connected neurons which receive more than one input per cycle from presynaptic neurons. The novelty of our results consists of a general approach to phase resetting in neural cells. At the same time, we proved that there is no need to change the traditional (single-stimulus) PRC protocol since multiple stimuli PRCs can be readily expressed in terms of the traditional single-stimulus PRC.

We found that the predicted two-stimulus PRC matches the experimental PRC. A critical evaluation of this very important and novel result in the theory of phase resetting must start from our assumptions. First, we assumed instantaneous resetting, i.e. the effect of the first stimulus is consumed by the time the second stimulus arrives. This assumption allowed us to treat the second stimulus as if it acts alone on a neural oscillator and re-use the single-stimulus PRC, hence the name iterative multiple stimuli PRC method. The assumption definitely stands for a wide class of neural oscillators characterized by a so-called "infinitely attractive limit cycle" [1]. For such neural oscillators, a small perturbation from the unperturbed phase space trajectory quickly disappears over a time interval much shorter than the intrinsic firing period of the neuron. "Infinitely attractive limit cycle" occur close to a saddle-node bifurcation that generates a type I excitability [8,9,10,11]. However, for type II excitability class, which is determined by a Poincare-Andronov-Hopf bifurcation [8,9,10,11], the system does not always return quickly to its unperturbed state. This is the reason we tested our theory in the worst case scenario by using a type II Morris-Lecar model neuron. Although we did not carry out an exhaustive search of the entire parameter space to prove that our theoretical prediction is correct, the parameters selected here are representative and the estimation error is reasonably low (below 5%). It would be very hard to improve the precision of prediction formula beyond the current values due to intrinsic limitations posed by this first assumption. Indeed, the validity of this assumption is determined by the detailed ionic mechanisms of the individual neuron. While some neurons, such as type I, would generally fulfill the requirements, it is well known that type II neurons have parameter ranges where they relax very slowly to the unperturbed state [1,3].

The second assumption was that PRC scales with the firing period. While it would be very hard to improve the precision of prediction formula by working on the first assumption, the second assumption could be eliminated completely. It is obviously convenient to assume that the single-stimulus PRC looks identical for different firing period. However, experimentally measuring single-stimulus PRC is equally convenient, which eliminates any potential error induced by the second assumption.

The method of PRC has obvious limitations beyond the two assumptions that limit the accuracy of two-stimulus PRC prediction. For example, it cannot be applied to designing a new and very specific drug targeting a neurodegenerative disease. In such a case, the model would need to capture all the details of neural activity and describe specific ion channels up to the morphology of the cell. However, our goal is to understand how neurons communicate and produce coherent activity at neural network level. For such an endeavor a simple input-output transfer function, such as the single-stimulus PRC, suffices.

**Acknowledgements**

This research was supported through NSF-CAREER award IOS 1054914.

## Notes and references

**Corresponding author E-mail: OprisanS@cofc.edu*

1. Ermentrout GB. 1996. Type I Membranes, Phase Resetting Curves, and Synchrony. Neural Computation 8(5): 979-1001.
2. Folgering JHA, Reza S-N, Dedman A, Patel A, Delmas P, Honor E. 2008. Molecular Basis of the Mammalian Pressure-sensitive Ion Channels: Focus on Vascular Mechanotransduction. Progress in Biophysics and Molecular Biology 97(2-3): 180-95.
3. Galn RF, Ermentrout GB, Urban NN. 2005. Efficient Estimation of Phase-Resetting Curves in Real Neurons and Its Significance for Neural-Network Modeling. Phys. Rev. Lett. 94(15).
4. Hodgkin A, Huxley A. 1952. A Quantitative Description of Membrane Current and Its Application to Conduction and Excitation in Nerve. J. Physiol. 117: 500-544.
5. Kandel ER, Schwartz JH, Jessell TM. 2000. Principles of Neural Science. McGraw-Hill, Health Professions Division, New York:.
6. Kullmann DM, Waxman SG. 2010. Neurological Channelopathies: New Insights into Disease Mechanisms and Ion Channel Function. J. Physiol. 588(11): 1823-827.